

Astrophysics and Space Science Library 461

Tomaso M. Belloni
Mariano Méndez
Chengmin Zhang
Editors

Timing Neutron Stars: Pulsations, Oscillations and Explosions

 Springer

Astrophysics and Space Science Library

Volume 461

Series Editor

Steven N. Shore, Dipartimento di Fisica “Enrico Fermi”, Università di Pisa,
Pisa, Italy

The Astrophysics and Space Science Library is a series of high-level monographs and edited volumes covering a broad range of subjects in Astrophysics, Astronomy, Cosmology, and Space Science. The authors are distinguished specialists with international reputations in their fields of expertise. Each title is carefully supervised and aims to provide an in-depth understanding by offering detailed background and the results of state-of-the-art research. The subjects are placed in the broader context of related disciplines such as Engineering, Computer Science, Environmental Science, and Nuclear and Particle Physics. The ASSL series offers a reliable resource for scientific professional researchers and advanced graduate students.

Series Editor:

STEVEN N. SHORE, Dipartimento di Fisica “Enrico Fermi”, Università di Pisa, Pisa, Italy

Advisory Board:

F. BERTOLA, University of Padua, Italy

C. J. CESARSKY, Commission for Atomic Energy, Saclay, France

P. EHRENFREUND, Leiden University, The Netherlands

O. ENGVOLD, University of Oslo, Norway

E. P. J. VAN DEN HEUVEL, University of Amsterdam, The Netherlands

V. M. KASPI, McGill University, Montreal, Canada

J. M. E. KUIJPERS, University of Nijmegen, The Netherlands

H. VAN DER LAAN, University of Utrecht, The Netherlands

P. G. MURDIN, Institute of Astronomy, Cambridge, UK

B. V. SOMOV, Astronomical Institute, Moscow State University, Russia

R. A. SUNYAEV, Max Planck Institute for Astrophysics, Garching, Germany

More information about this series at <http://www.springer.com/series/5664>

Tomaso M. Belloni • Mariano Méndez •
Chengmin Zhang
Editors

Timing Neutron Stars: Pulsations, Oscillations and Explosions

 Springer

Editors

Tomaso M. Belloni
INAF Osservatorio Astronomico di Brera
Merate, Italy

Mariano Méndez
Kapteyn Astronomical Institute
University of Groningen
Groningen, The Netherlands

Chengmin Zhang
National Astronomical Observatories
and
The University of Chinese Academy
of Sciences
Chinese Academy of Sciences
Beijing, China

ISSN 0067-0057 ISSN 2214-7985 (electronic)
Astrophysics and Space Science Library
ISBN 978-3-662-62108-0 ISBN 978-3-662-62110-3 (eBook)
<https://doi.org/10.1007/978-3-662-62110-3>

© Springer-Verlag GmbH Germany, part of Springer Nature 2021

This work is subject to copyright. All rights are reserved by the Publisher, whether the whole or part of the material is concerned, specifically the rights of translation, reprinting, reuse of illustrations, recitation, broadcasting, reproduction on microfilms or in any other physical way, and transmission or information storage and retrieval, electronic adaptation, computer software, or by similar or dissimilar methodology now known or hereafter developed.

The use of general descriptive names, registered names, trademarks, service marks, etc. in this publication does not imply, even in the absence of a specific statement, that such names are exempt from the relevant protective laws and regulations and therefore free for general use.

The publisher, the authors, and the editors are safe to assume that the advice and information in this book are believed to be true and accurate at the date of publication. Neither the publisher nor the authors or the editors give a warranty, expressed or implied, with respect to the material contained herein or for any errors or omissions that may have been made. The publisher remains neutral with regard to jurisdictional claims in published maps and institutional affiliations.

Cover illustration: Composite image showing an artist's impression of the SGR 1806-20 magnetar during its giant flare in 2004. The magnetic field lines are shown, together with the presence of hot spots. These are responsible for the oscillations that can be seen in the overlaid light curve shown in yellow. The time axis spans about six minutes. Artist's Image credit: NASA Light curve credit: T. Belloni

This Springer imprint is published by the registered company Springer-Verlag GmbH, DE part of Springer Nature.

The registered company address is: Heidelberger Platz 3, 14197 Berlin, Germany

Preface

The study of neutron stars is important in several aspects. On the astrophysical side, from their birth from supernova events to their evolution when isolated or in binary systems, they constitute an important end point of stellar evolution. In accreting binaries, they provide an important class of objects for our understanding of accretion onto compact objects, together with black-hole binaries. We now know transitional objects between accreting neutron stars and radio pulsars that can help us understand better both classes of sources. On the physical side, they constitute formidable and unique laboratories to study fundamental processes. First, they are the only objects in the Universe where matter is at extremely high density and we still do not know the associated equation of state. Second, they offer us the possibility to study their internal structure, affected by high angular momentum and large magnetic field. Third, but not least, they are being used as test objects for experimental measurements of the effects of general relativity (GR). Binary pulsars provide very precise clocks to monitor the orbit of the object and detect modifications due to GR, while in accreting neutron stars the strength of the gravitational field close to the compact object modifies the properties of accretion giving us the possibility to study GR in the strong-field regime.

All these studies are based on the time variability of the flux, from the radio band to X-rays. This book is focused on timing aspects. As the title says, this variability is in three forms. Pulsations, observed historically from radio pulsars, but now detected also in accreting low-mass X-ray binaries, the progenitors of millisecond pulsars. Oscillations, from the noisy variability of accreting systems, where strong quasi-periodicities are observed at a period of a few milliseconds, comparable to the dynamical time close to the surface of the neutron star. Explosions, powerful nuclear-powered X-ray bursts that take place on the surface of accreting neutron stars when the accretion level is in the favorable range.

Merate, Italy
Groningen, The Netherlands
Beijing, China
June 2020

Tomaso M. Belloni
Mariano Méndez
Chengmin Zhang

Contents

1	Astrophysical Constraints on Dense Matter in Neutron Stars	1
	M. Coleman Miller	
1.1	Introduction	2
1.2	Expectations from Nuclear Theory	3
1.2.1	The Basics: Dense Matter and Neutron Stars	3
1.2.2	Models of Matter at High Densities	6
1.2.3	Construction of Neutron Star Models from Microphysics	9
1.3	Constraints on Mass from Binary Observations	10
1.3.1	Newtonian Observations of Binaries	10
1.3.2	Post-Keplerian Measurements of Pulsar Binaries	11
1.3.3	Dynamically Estimated Neutron Star Masses and Future Prospects	13
1.4	Constraints on Radius, and Other Mass Constraints	15
1.4.1	Thermonuclear X-ray Bursts	15
1.4.2	Fits of Thermal Spectra to Cooling Neutron Stars	18
1.4.3	Modeling of Waveforms	22
1.4.4	Maximum Spin Rate	24
1.4.5	Kilohertz QPOs	25
1.4.6	Other Methods to Determine the Radius and Future Prospects	27
1.5	Cooling of Neutron Stars	28
1.5.1	The URCA Processes	29
1.5.2	Additional Neutrino Production Channels and Suppression	30
1.5.3	Photon Luminosity and the Minimal Cooling Model	31
1.5.4	Observations and Systematic Errors	32
1.5.5	Current Status and Future Prospects	33
1.6	Gravitational Waves from Coalescing Binaries	34
1.7	Summary	37
	References	39

2	General Relativity Measurements from Pulsars	53
	Marta Burgay, Delphine Perrodin, and Andrea Possenti	
2.1	Why Radio Pulsars	54
2.2	The Many Faces of the Radio Pulsar Zoo	55
2.2.1	Radio Pulsars	55
2.2.2	Intermittent Pulsars	59
2.2.3	Rotating RADIO Transients	61
2.3	Relativistic Binary Pulsars	62
2.3.1	Basic Evolution	62
2.3.2	The Current Sample	66
2.4	Pulsar Timing Basics	72
2.4.1	Timing Procedure: Measurement of the ToAs	72
2.4.2	Timing Procedure: Modelling the ToAs	74
2.5	Probing Relativistic Gravity with Pulsars	78
2.5.1	Tests Using PPN Parameters	80
2.5.2	Tests Using PK Parameters	82
2.5.3	Future Prospects.....	88
	References	90
3	Magnetars: A Short Review and Some Sparse Considerations	97
	Paolo Esposito, Nanda Rea, and Gian Luca Israel	
3.1	Historical Overview	98
3.2	Observational Characteristics	99
3.2.1	Persistent Emission	99
3.2.2	Transient Activity	103
3.2.3	Magnetar Formation	116
3.2.4	Magnetic Field Evolution and the Neutron Star Bestiary	117
3.2.5	Low- <i>B</i> Magnetars and High- <i>B</i> Pulsars	120
3.2.6	Magnetars in Binary Systems	124
3.3	Final Remarks.....	126
	References	127
4	Accreting Millisecond X-ray Pulsars	143
	Alessandro Patruno and Anna L. Watts	
4.1	Introduction	144
4.2	The Accreting Millisecond X-ray Pulsar Family	146
4.2.1	Intermittency	149
4.3	Observations of the AMXPs	151
4.3.1	SAX J1808.4-3658.....	151
4.3.2	XTE J1751-305	156
4.3.3	XTE J0929-314	158
4.3.4	XTE J1807-294	158
4.3.5	XTE J1814-338	159
4.3.6	IGR J00291+5934	160
4.3.7	HETE J1900.1-2455	161

4.3.8	Swift J1756.9-2508	162
4.3.9	Aql X-1	163
4.3.10	SAX J1748.9-2021	164
4.3.11	NGC 6440 X-2	165
4.3.12	IGR J17511-3057	165
4.3.13	Swift J1749.4-2807	166
4.3.14	IGR J17498-2921	167
4.3.15	IGR J18245-2452	167
4.4	Accretion Torques	168
4.4.1	Coherent Timing Technique	172
4.4.2	Observations: Accretion Torques in AMXPs	175
4.5	Pulse Profiles	180
4.5.1	Pulse Fractional Amplitudes and Phase Lags	180
4.5.2	Pulse Shape Evolution	182
4.6	Long Term Evolution and Pulse Formation Process	183
4.6.1	Specific Sources	183
4.6.2	The Maximum Spin Frequency of Neutron Stars	186
4.6.3	Why Do Most Low Mass X-ray Binaries Not Pulsate?	187
4.7	Thermonuclear Bursts	189
4.8	Aperiodic Variability and kHz QPOs	194
4.9	Open Problems and Final Remarks	196
	References	197
5	Thermonuclear X-ray Bursts	209
	Duncan K. Galloway and Laurens Keek	
5.1	Overview	210
5.1.1	Theory of Burst Ignition and Nuclear Burning Regimes	211
5.1.2	Status of Burst Observations	217
5.2	X-ray Burst Ignition	221
5.2.1	Thin-Shell Instability and Electron Degeneracy	222
5.2.2	Reignition After a Short Recurrence Time	222
5.2.3	Ignition Latitude	224
5.3	The Burst Spectral Energy Distribution	225
5.3.1	The Continuum Spectrum	225
5.3.2	Discrete Spectral Features	228
5.4	Interaction with the Accretion Environment	230
5.4.1	Reflection by the Accretion Disk	233
5.4.2	Anisotropic Emission	234
5.5	Burst Oscillations and the Neutron Star Spin	235
5.6	mHz Oscillations and Marginally Stable Burning	236
5.6.1	Observations of mHz QPOs	237
5.6.2	Theoretical Interpretation: Marginally Stable Burning	238

5.7	Burst Duration and Fuel Composition	239
5.7.1	Intermediate Duration Bursts	240
5.7.2	Superbursts	242
5.8	Thermonuclear Burst Simulations	244
5.8.1	Single-Zone Models	245
5.8.2	One-Dimensional Multi-Zone Models	245
5.8.3	Multi-Dimensional Models	248
5.9	Nuclear Experimental Physics	249
5.10	Summary and Outlook	251
	References	252
6	High-Frequency Variability in Neutron-Star Low-Mass X-ray	
	Binaries	263
	Mariano Méndez and Tomaso M. Belloni	
6.1	Introduction	264
6.2	History	264
6.3	Basic Frequencies Close to a Neutron Star	266
6.4	Timing Phenomenology: QPOs 101	267
6.5	Linking Observed Frequencies with Theoretical Expectations	282
6.6	QPO Frequency Correlations	286
6.7	Relation Between Properties of the kHz QPOs and Parameters of the Energy Spectrum	287
6.8	Beyond QPO Frequencies	291
6.8.1	The Fractional rms Amplitude of the kHz QPOs	291
6.8.2	The Width of the kHz QPOs	298
6.8.3	The Energy-Dependent Lags and Coherence of the kHz QPOs	305
6.8.4	Other Phenomenology of the kHz QPOs	315
6.9	Probing Neutron-Star Interiors and GR with kHz QPO	319
6.10	Conclusions and Outlook	320
	References	321
	Index	333

Contributors

Tomaso M. Belloni INAF - Osservatorio Astronomico di Brera, Merate, Italy

Marta Burgay INAF-Osservatorio Astronomico di Cagliari, Selargius, CA, Italy

Paolo Esposito Scuola Universitaria Superiore IUSS Pavia, Pavia, Italy
INAF - Istituto di Astrofisica Spaziale e Fisica Cosmica di Milano, Milano, Italy

Duncan K. Galloway School of Physics & Astronomy, Monash University, Clayton, VIC, Australia

Gian Luca Israel Osservatorio Astronomico di Roma, INAF, Monteporzio Catone, Rome, Italy

Laurens Keek CRESST and X-ray Astrophysics Laboratory NASA/GSFC, Greenbelt, MD, USA
Department of Astronomy, University of Maryland, College Park, MD, USA

Mariano Méndez Kapteyn Astronomical Institute, University of Groningen, Groningen, The Netherlands

M. Coleman Miller Department of Astronomy and Joint Space-Science Institute, University of Maryland, College Park, MD, USA

Alessandro Patrino Institute of Space Sciences, CSIC (Consejo Superior de Investigaciones Científicas), Barcelona, Spain

Delphine Perrodin INAF-Osservatorio Astronomico di Cagliari, Selargius, CA, Italy

Andrea Possenti INAF-Osservatorio Astronomico di Cagliari, Selargius, CA, Italy

Nanda Rea Institute of Space Sciences (ICE, CSIC), Barcelona, Spain
Institut d’Estudis Espacials de Catalunya (IEEC), Barcelona, Spain
Astronomical Institute “Anton Pannekoek”, University of Amsterdam, Amsterdam,
The Netherlands

Anna L. Watts Astronomical Institute “Anton Pannekoek”, University of
Amsterdam, Amsterdam, The Netherlands

Chapter 1

Astrophysical Constraints on Dense Matter in Neutron Stars



M. Coleman Miller

Contents

1.1	Introduction	2
1.2	Expectations from Nuclear Theory	3
1.2.1	The Basics: Dense Matter and Neutron Stars	3
1.2.2	Models of Matter at High Densities	6
1.2.3	Construction of Neutron Star Models from Microphysics	9
1.3	Constraints on Mass from Binary Observations	10
1.3.1	Newtonian Observations of Binaries	10
1.3.2	Post-Keplerian Measurements of Pulsar Binaries	11
1.3.3	Dynamically Estimated Neutron Star Masses and Future Prospects	13
1.4	Constraints on Radius, and Other Mass Constraints	15
1.4.1	Thermonuclear X-ray Bursts	15
1.4.2	Fits of Thermal Spectra to Cooling Neutron Stars	18
1.4.3	Modeling of Waveforms	22
1.4.4	Maximum Spin Rate	24
1.4.5	Kilohertz QPOs	25
1.4.6	Other Methods to Determine the Radius and Future Prospects	27
1.5	Cooling of Neutron Stars	28
1.5.1	The URCA Processes	29
1.5.2	Additional Neutrino Production Channels and Suppression	30
1.5.3	Photon Luminosity and the Minimal Cooling Model	31
1.5.4	Observations and Systematic Errors	32
1.5.5	Current Status and Future Prospects	33
1.6	Gravitational Waves from Coalescing Binaries	34
1.7	Summary	37
	References	39

M. C. Miller (✉)

Department of Astronomy and Joint Space-Science Institute, University of Maryland, College Park, MD, USA

e-mail: miller@astro.umd.edu

Abstract Ever since the discovery of neutron stars it has been realized that they serve as probes of a physical regime that cannot be accessed in laboratories: strongly degenerate matter at several times nuclear saturation density. Existing nuclear theories diverge widely in their predictions about such matter. It could be that the matter is primarily nucleons, but it is also possible that exotic species such as hyperons, free quarks, condensates, or strange matter may dominate this regime. Astronomical observations of cold high-density matter are necessarily indirect, which means that we must rely on measurements of quantities such as the masses and radii of neutron stars and their surface effective temperatures as a function of age. Here we review the current status of constraints from various methods and the prospects for future improvements.

1.1 Introduction

The nature of the matter in the cores of neutron stars is of great interest to nuclear physicists and astrophysicists alike, but its properties are difficult to establish in terrestrial laboratories. This is because neutron star cores reach a few times the density of matter in terrestrial nuclei and yet they are strongly degenerate and they have far more neutrons than protons. The core matter thus occupies a different phase than is accessible in laboratories. Within current theoretical uncertainties there are many possibilities for the state of this matter: it could be primarily nucleonic, or dominated by deconfined quark matter, or mainly hyperons, or even mostly in a condensate.

Only astrophysical observations of neutron stars can constrain the properties of the cold supranuclear matter in their cores. Because we cannot sample the matter directly, we need to infer its state by measurements of neutron star masses, radii, and cooling rates. For the last two of these, the method of measurement is highly indirect and thus subject to systematic errors. Note, to be precise, that throughout this review we mean by mass the gravitational mass (which would be measured by using Kepler's laws for a satellite in a distant orbit around the star) rather than the baryonic mass (which is the sum of the rest masses of the individual particles in the star); for a neutron star, the gravitational mass is typically less than the baryonic mass by $\sim 20\%$. We also mean by radius the circumferential radius, i.e., the circumference at the equator divided by 2π , rather than other measures such as the proper distance between the stellar center and a point on the surface. Again, for objects as compact as neutron stars, the difference can amount to tens of percent.

In this review we discuss current attempts to measure the relevant stellar properties. We also discuss future prospects for constraints including those that will come from analysis of gravitational waves. For each of the constraint methods, we discuss the current uncertainties and assess the prospects for lowering systematic errors in the future. In Sect. 1.2 we set the stage by discussing current expectations from nuclear theory and laboratory measurements. In Sect. 1.3 we examine mass measurements in binaries. In Sect. 1.4 we discuss current attempts to measure

the radii of neutron stars and show that most of them suffer severely from systematic errors. In Sect. 1.5 we explore what can be learned from cooling of neutron stars, and the difficulties in getting clean measurements of temperatures. In Sect. 1.6 we investigate the highly promising constraints that could be obtained from the detection of gravitational waves from neutron star–neutron star or neutron star–black hole systems. We summarize our conclusions in Sect. 1.7. For other recent reviews of equation of state constraints from neutron star observations, see [27, 101, 116, 117, 129, 165, 171, 199, 206, 234].

1.2 Expectations from Nuclear Theory

Any observations of neutron stars bearing on the properties of high-density matter must be put into the context of existing nuclear theory. This theory, which relies primarily on laboratory measurements of matter at nuclear density that has approximately equal numbers of protons and neutrons, must be extrapolated significantly to the asymmetric matter at far higher density in the cores of neutron stars. We also note that the inferred macroscopic properties of neutron stars depend on the nature of strong gravity as well as on the properties of dense matter (e.g., [183]), but for this review we will assume the correctness of general relativity.

In this section we give a brief overview of current thinking about dense matter. We begin with simple arguments motivating the zero-temperature approximation for the core matter and giving the basics of degenerate matter. We then address a commonly-asked question: given that the fundamental theory of quantum chromodynamics (QCD) exists, why can we not simply employ computer calculations (e.g., using lattice gauge theory) to determine the state of matter at high densities? Given that in fact such calculations are not practical, we explore the freedom that exists in principle to construct models of high-density matter; the fundamental point is that because the densities are well above what is measurable in the laboratory, one could always imagine, in the context of a model, adding terms that are negligible at nuclear density or for symmetric matter but important when the matter is a few times denser and significantly asymmetric. After discussing some example classes of models, we survey current constraints from laboratory experiments and future prospects. We conclude with a discussion of how one would map an idealized future data set of masses, radii, temperatures, etc. of neutron stars onto the equation of state of cold dense matter.

1.2.1 *The Basics: Dense Matter and Neutron Stars*

Consider a set of identical fermions (e.g., electrons or neutrons) of mass m and number density n . The linear space available to each fermion is thus $\Delta x \sim n^{-1/3}$, and the uncertainty principle states that the uncertainty in momentum (and hence the minimum momentum) is given by $\Delta p \Delta x \sim \hbar$ and thus $p_{\min} \sim \hbar n^{1/3}$, where

$\hbar = 1.05457 \times 10^{-27}$ erg s is the reduced Planck constant. Done more precisely and assuming isotropic matter we find that this minimum is the Fermi momentum $p_F = (3\pi^2 \hbar^3 n)^{1/3}$. The Fermi energy adds to the rest-mass energy via $E_{\text{tot}} = (m^2 c^4 + p_F^2 c^2)^{1/2} = mc^2 + E_F$, and is $E_F \approx p_F^2/2m$ for $p_F \ll mc$ and $E_F \approx p_F c$ for $p_F \gg mc$, where $c = 2.99792458 \times 10^{10}$ cm s⁻¹ is the speed of light.

Matter is degenerate when $E_F > kT$, and strongly degenerate when $E_F \gg kT$, where $k = 1.38065 \times 10^{-16}$ erg K⁻¹ is the Boltzmann constant and T is the temperature. As a result, electrons (with their low masses $m_e = 9.109382 \times 10^{-28}$ g = 0.510999 MeV/c²) become degenerate at much lower densities than do neutrons or protons. Matter dominated by nuclei heavier than hydrogen has ~ 2 baryons per electron, and hence electrons become relativistically degenerate ($p_F = m_e c$) at a density of $\approx 2 \times 10^6$ g cm⁻³. In addition, above $\approx 2.5 \times 10^7$ g cm⁻³ the total energy of electrons becomes larger than $m_n c^2 - m_p c^2 = 1.294$ MeV, where $m_n = 1.674927 \times 10^{-24}$ g = 939.566 MeV/c² and $m_p = 1.672622 \times 10^{-24}$ g = 938.272 MeV/c² are respectively the rest masses of neutrons and protons. As a result, at these and greater densities electrons and protons can undergo inverse beta decay $e^- + p \rightarrow n + \nu_e$. At higher densities the ratio of neutrons to protons in nuclei increases, and then at the “neutron drip” density $\rho_{nd} \approx 4.3 \times 10^{11}$ g cm⁻³ neutrons are stable outside nuclei. The neutron drip density is derived in detail in, e.g., [22], but a good estimate can be obtained by a simple argument. Neutrons can drip out of the nucleus when the total electron energy per nucleon equals the nuclear binding energy per nucleon (as described in [22] there are small corrections due to lattice energy and the nonzero energy of neutron continuum states). The binding energy per nucleon is ~ 8 MeV (see, e.g., Table 3 of [22]). At high densities, $Z/A \sim 0.3$ in contrast to the $Z/A \sim 0.5$ common at lower densities. Thus the condition on the electron Fermi energy for neutron drip is $E_{F,e} \approx 8(A/Z)$ MeV. The density at which this happens is therefore approximately 2×10^6 g cm⁻³ $(0.5/0.3)[(8 \text{ MeV}/0.3)/0.5 \text{ MeV}]^3 \approx 4 \times 10^{11}$ g cm⁻³, where we extrapolate from the density at which the electron Fermi energy becomes relativistic.

At infinite density, equilibrium matter consisting of just neutrons, protons, and electrons would have eight times as many neutrons as protons (and electrons, because charge balance has to be maintained). To see this, note that at infinite density all species are ultrarelativistic and their chemical potentials are thus dominated by their Fermi energies. Charge balance means that $n_p = n_e$, so equilibrium implies

$$\begin{aligned} E_{F,n} &= E_{F,p} + E_{F,e^-} \\ &= 2E_{F,p} \\ n_n^{1/3} &= 2n_p^{1/3} \\ n_n &= 8n_p . \end{aligned} \tag{1.1}$$

For a neutron star with a canonical mass $M = 1.4 M_\odot$ (where $M_\odot = 1.989 \times 10^{33}$ g is the mass of the Sun) and radius $R = 10$ km that for simplicity we will treat as made entirely of free neutrons, the average number density is $n = (M/m_n)/(4\pi R^3/3) = 4 \times 10^{38}$ cm⁻³. This implies $p_F = 2.4 \times 10^{-14}$ g cm s⁻¹ and thus $E_F \approx 2 \times 10^{-4}$ erg = 100 MeV. This corresponds to a temperature of

$T_F = E_F/k \approx 10^{12}$ K, which is much hotter than the expected interior temperatures $T < 10^{10}$ K typical of neutron stars more than a few years old [172]. Neutron stars are strongly degenerate.

Note, however, that the high Fermi energy of neutrons suggests the possibility of additional particles at high densities. For example, the lambda particle has a rest mass of $m_\Lambda = 1115.6 \text{ MeV}/c^2$, so if the neutron Fermi energy exceeds 176 MeV then the lambda is in principle stable because 176 MeV plus the neutron rest-mass energy 939.6 MeV exceeds 1115.6 MeV. Several other particles are within $300 \text{ MeV}/c^2$ of the neutron. In addition, because the density at the center of a neutron star is a few times nuclear saturation density $\rho_{\text{nuc}} \approx 2.6 \times 10^{14} \text{ g cm}^{-3}$, quarks may become deconfined or matter might transition to a state that is lower-energy than nucleonic matter even at zero pressure (strange matter; see, e.g., [77]). Various density thresholds are summarized in Fig. 1.1.

Stars supported by nonrelativistic degeneracy pressure (a reasonable approximation for neutron stars, because $E_F < m_n c^2$) have radii that decrease with increasing mass in contrast to most other objects. To see this, consider a star with a mass M and radius R supported by nonrelativistic fermions of mass m . The Fermi energy per particle is $E_F \sim p_F^2/2m \sim \hbar^2 n^{2/3} \sim (M/R^3)^{2/3} \sim M^{2/3}/R^2$. The gravitational

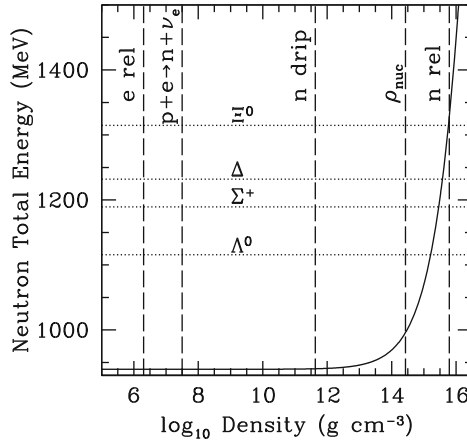


Fig. 1.1 Total energy per free neutron versus mass density (solid line). Above $\sim 10^{13} \text{ g cm}^{-3}$ the Fermi energy starts to contribute palpably to the total, and above $\sim 10^{15} \text{ g cm}^{-3}$ the total energy can exceed the rest mass energy of particles such as Λ^0 , Σ^+ , Δ , and Ξ^0 (marked by horizontal dotted lines). Interactions between these particles can change the threshold density. The central densities of realistic neutron stars range from $\sim 5 \times 10^{14} \text{ g cm}^{-3}$ to $\sim \text{few} \times 10^{15} \text{ g cm}^{-3}$, so some of these exotic particles may indeed be energetically favorable. Also marked are the densities at which free electrons become relativistic; where those electrons have enough total energy to make $p + e^- \rightarrow n + \nu_e$ possible; where free neutrons can exist stably (i.e., at neutron drip); nuclear saturation density ρ_{nuc} ; and where free neutrons have a Fermi energy equal to their rest-mass energy. To calculate the neutron Fermi energy we assume that all the mass is in free neutrons; in reality at least a few percent of the mass is in protons and other particles, and below ρ_{nuc} a significant fraction of mass is in nuclei

energy per particle is $E_G \sim -GMm/R$, where $G = 6.67 \times 10^{-8} \text{ g}^{-1} \text{ cm}^3 \text{ s}^{-2}$ is Newton's gravitational constant, so the total energy per particle is $E_{\text{tot}} = C_1 M^{2/3}/R^2 - C_2 M/R$ where C_1 and C_2 are constants. Minimizing with respect to R gives $R \sim M^{-1/3}$. Effects associated with interactions can change this slightly, but in practice most equations of state produce a radius that either decreases with increasing mass or is nearly constant over a broad range in mass. This led [130] to note that even for a star of unknown mass a measurement of the radius to within $\sim 10\%$ would provide meaningful constraints on the equation of state.

1.2.2 Models of Matter at High Densities

There are several classes of matter beyond nuclear density: ones in which neutrons and protons are the only baryons, ones in which other baryons enter (especially those with strange quarks), ones involving deconfined quark matter, and so on. Within each class there are a number of adjustable parameters, some of which are constrained by laboratory measurements at nuclear density or below but many of which can be changed to accommodate observations of neutron stars.

When confronted by this complexity a common question is: why is there uncertainty about dense matter? The fundamental theory, QCD, is well-established. Asymptotic freedom is not reached at neutron star densities, so the coupling constant is large enough that expansions similar to those in quantum electrodynamics are not straightforward, but in principle one could imagine Monte Carlo calculations that establish the ground state of degenerate high-density matter.

This approach is unfortunately not currently practical, due to the lack of a viable algorithm for high baryon densities. This is because of the so-called “fermion sign problem”, which has been known for many years. We start by considering a representative but small volume of matter at some density and chemical potential μ that can exchange energy and particles with its surroundings but has a fixed volume [109]. The thermodynamic state of the matter is therefore described by a grand canonical ensemble using a partition function

$$Z = Z(T, \mu) = \text{Tr} \{ \exp[-(\mathcal{H} - \mu N)/kT] \} \quad (1.2)$$

where \mathcal{H} is the Hamiltonian and N is the particle number operator. It is common to use $\beta \equiv 1/(kT)$. The trace is evaluated over Fock space, which makes this formulation inconvenient. One can instead rewrite Z as

$$Z = \int \mathcal{D}A \det M(A) e^{-S_G(A)}, \quad (1.3)$$

that is, as a Euclidean functional integral over classical field configurations. Here A represents the degrees of freedom (quarks, gluons, ...), $S_G(A; \beta) = \int_0^\beta dx^4 \int d^3x \mathcal{L}_G^E(A)$ is the thermal Euclidean gauge action, and the quark propagator matrix is $M(A) = \not{D}(A) - m - \mu \gamma_4$ where $\not{D} = \gamma_\mu (\partial_\mu - ig A_\mu^a t^a)$, t^a are

the Hermitian group generators, g is the strong coupling constant, and γ are the Euclidean gamma matrices.

For a vanishing chemical potential $\mu = 0$, $\det M(A)$ is positive definite, meaning that all contributions add in the same direction and Z is comparatively straightforward to compute. If instead μ is real and nonzero, then $\det M(A)$ is complex in general. Thus although Z is still real and strictly positive, the integrands have various phases and the integral takes the form of a cancellation between large quantities. The bad news is that the general fermion sign problem is NP-hard [216], but work is proceeding on better approximation methods. If a first-principles evaluation of Z yields, without ambiguity, the equilibrium state of dense matter at low temperatures, then measurements of the properties of neutron stars would serve as important tests of QCD itself and would thus be probes of very fundamental physics indeed. Until that point, however, it is necessary to use phenomenological models.

It is very difficult to rule out an entire class of models (e.g., those with only nucleonic degrees of freedom or those with significant contributions from hyperons). This is because neutron star core densities and the asymmetry in the number densities of neutrons and protons are significantly greater than those that can be probed in laboratories. As a result, one could always imagine adding contributions that involve high powers of the density or asymmetry. These contributions would have a negligible impact on laboratory matter but would have important effects in the cores of neutron stars. One can make some general statements: for instance, if non-nucleonic components become important above some density the equilibrium radius at a given mass and the maximum mass both tend to be smaller than if only nucleonic degrees of freedom contribute (because the presence of a new energetically favorable composition softens the equation of state). Unfortunately, it is difficult to establish a particular mass or radius that would eliminate such exotic models. For example, hyperonic and hybrid quark models of neutron stars have been constructed with maximum masses $> 2.0 M_\odot$ [117, 122]. Nonetheless, although neutron star observations cannot entirely rule out model classes in principle, their role is important because they probe a different realm of matter than what is accessible in laboratories. Ockham's razor should then be used to judge between different model classes: if one class fits all data using a small number of parameters that have reasonable values and other classes require great complexity or unreasonable values, the first class would be preferred.

One basic category of models, relativistic mean field theories, is quite phenomenological in nature. In these models the degrees of freedom are nucleons and mesons (which couple minimally to the nucleons but the coupling could have some density dependence). The coupling strengths can be adjusted to laboratory data and/or neutron star observations. In a more microscopically oriented approach, one starts instead from some given nucleon-nucleon interaction (which can be extended to more than two nucleons) that is fitted to data including the binding energy of light nuclei and scattering data (for a recent effort in the context of chiral effective field theory, see [99]). In both approaches there is considerable freedom about the types of particles considered, e.g., the particles could be nucleons or the particles could

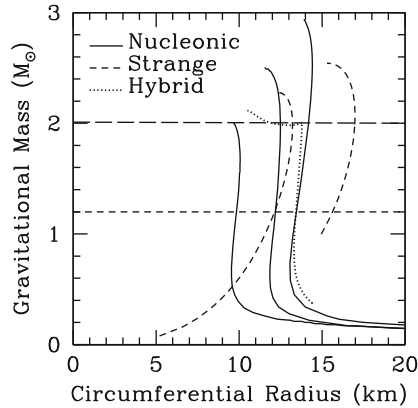


Fig. 1.2 Mass versus radius for nonrotating stars constructed using several different high-density equations of state. Rotation changes the radius to second order in the spin rate, but the corrections are minor for known neutron stars. The solid curves include only nucleonic degrees of freedom (these are the mass-radius relations for the soft, medium, and hard equations of state from [100]), the short dashed lines assume bare strange matter [121], and the dotted curve uses a hybrid quark equation of state with a phase transition [34]. The horizontal dashed line at $1.2 M_{\odot}$ represents approximately the minimum gravitational mass for a neutron star in current formation scenarios, whereas the horizontal dashed line at $2.01 M_{\odot}$ shows the highest precisely measured gravitational mass for a neutron star

include hyperons or deconfined quarks. We plot some mass-radius relations from representative equations of state in Fig. 1.2. It is clear that models can be constrained tightly if more massive neutron stars are discovered, or if neutron star radii can be measured with accuracy and precision (especially for stars of known mass).

Constraints on the equation of state of cold dense matter can be obtained from astronomical observations or laboratory experiments. Some of the more useful experimental data come from relativistic heavy-ion collisions, which can reach 2 to 4.5 times nuclear saturation density [70] but which have relativistic temperatures and are therefore not degenerate. In addition, in such collisions the time for weak interactions to occur is short, in contrast to the effectively infinite time available in neutron stars. Laboratory data also include the binding energies of light nuclei and recent measurements of the neutron skin thickness of heavy nuclei such as ^{208}Pb ($0.33^{+0.16}_{-0.18}$ fm according to the PREX team [3]; see [178] for some of the implications of the expected more precise future measurements), which provide a rare glimpse of neutron-rich matter because the neutron wavefunctions extend slightly beyond the proton wavefunctions. These experiments thus measure the microphysics semi-directly, whereas all astrophysical observations place indirect constraints. In order to make explicit contact between microphysics and astrophysics we now discuss briefly how to construct models of neutron stars given a high-density equation of state.

1.2.3 Construction of Neutron Star Models from Microphysics

We argued earlier that the Fermi energy in the cores of neutron stars is much greater than the thermal energy. If we also assume that the matter is in its ground state at a given density, this implies that the pressure is only a function of density: $P = P(\rho)$ (this is called a *barotropic* equation of state). If we have such an equation of state we can compute the structure of a nonrotating and hence spherically symmetric star using the Tolman-Oppenheimer-Volkoff (TOV) equation [164]:

$$\frac{dP(r)}{dr} = -\frac{G}{r^2} \left[\rho(r) + \frac{P(r)}{c^2} \right] \left[M(r) + 4\pi r^3 \frac{P(r)}{c^2} \right] \left[1 - \frac{2GM(r)}{c^2 r} \right]^{-1} \quad (1.4)$$

where $M(r) = \int_0^r 4\pi \rho(r) r^2 dr$ is the gravitational mass integrated from the center to a circumferential radius r . Note that for $P/c^2 \ll \rho$ and $GM/c^2 \ll r$ this reduces to the Newtonian equation of hydrostatic equilibrium $dP/dr = -GM\rho/r^2$. Thus one can construct a model star by choosing a central density or pressure and integrating to the surface, which is defined by $P = \rho = 0$. This gives the radius and gravitational mass of the star. Similar constructions are possible for stars that rotate uniformly or differentially in some specified manner (see [63, 207]), but it is conceptually clearer to focus on the nonrotating case.

One can therefore determine the neutron star mass-radius relation from a given equation of state. If we suppose that in the future we will have precise measurements of the radii and gravitational masses of a large number of neutron stars, say from the minimum possible to the maximum possible mass, then comparison of the observed $M - R$ curve with predicted curves will strongly constrain the parameters of a given class of models. But is it possible to go in the other direction, that is, could one take observed (M, R) pairs and infer $P(\rho)$ directly while remaining agnostic about the microphysics that produces the equation of state?

This is not trivial. One might imagine that the construction of $P(\rho)$ would proceed as follows. First, we assume that we know the equation of state up to nuclear saturation density ρ_{nuc} . Even in this first step we therefore make an extrapolation from the nearly symmetric nuclear matter in nuclei to the highly asymmetric matter in neutron stars. We use this equation of state to compute the mass M_s and radius R_s of a star with a central density of ρ_{nuc} . We then observe a star with a slightly larger mass than M_s . The microscopic unknowns would be the central density (slightly larger than nuclear saturation) and the pressure at that density, which our two measurements (of M and R) are sufficient to constrain. We then bootstrap $P(\rho)$ by measuring the mass and radius of successively more massive neutron stars.

The difficulty with this procedure is evident from Figure 11 of [4], which shows that a star whose central density is exactly nuclear saturation density has a total mass of only $\sim 0.1 M_\odot$. To get to the $M \approx 1.2 M_\odot$ minimum for neutron star masses [163, 237] requires densities that are more than twice nuclear saturation. We will thus be required to extrapolate well beyond known matter in density and

nuclear asymmetry to fit neutron star data. This is not fatal, because it means that we are simply comparing model predictions with data, but it does mean that $P(\rho)$ cannot be inferred blindly without models.

If additional assumptions are made, for example that between fiducial densities the equation of state is a polytrope $P \propto \rho^\gamma$, then [166] have shown that precise mass and radius measurements of as few as three neutron stars could suffice to give an empirically determined $P(\rho)$. The inferred $P(\rho)$ would then be compared with the predictions from microphysical equations of state. As discussed by [131], there are additional relatively model-independent constraints on the equation of state that one can infer from observations. For example, the typical radius of a neutron star scales as the quarter power of the pressure near nuclear saturation density, and the maximum density that can be reached in a neutron star is $\rho_{\max} \approx 1.5 \times 10^{16} \text{ g cm}^{-3} (M_\odot/M_{\max})^2$ if the maximum mass is M_{\max} .

Our final note about the theoretical predictions is that there are some phenomena that have little effect on the mass-radius relation but are important for other observables. For example, the existence of a proton superconducting gap can modify core cooling dramatically [172], but the predicted gap energies of $\sim 0.1 - 1 \text{ MeV}$ [172] are so small compared to the Fermi energy that the overall structure of neutron stars will be affected minimally. Thus if neutron star temperatures and ages, particularly those of isolated neutron stars, can be inferred reliably, then they will provide a beautiful complement to the mass and radius measurements that are emphasized more in this review.

1.3 Constraints on Mass from Binary Observations

Mass measurements of neutron stars in binaries provide the most certain of all constraints on the properties of cold high-density matter, particularly when the companion to the neutron star is also a neutron star and thus the system approaches the ideal of two point masses. In this section we discuss such measurements, beginning with what can be learned from purely Newtonian observations and moving on to the greater precision and breaking of degeneracies that are enabled by measurements of post-Keplerian parameters from systems involving pulsars.

1.3.1 Newtonian Observations of Binaries

The classical approach to mass measurements in binaries assumes that one sees periodic variation in the energy of spectral lines from one of the stars in the binary, which we will call star 1. The period of variation is the orbital period P_{orb} , the shape of the variation gives the eccentricity e of the orbit, and the magnitude K_1 (which has dimensions of speed) of the variation indicates the line-of-sight component of the orbital speed of star 1. Using Kepler's laws these observed quantities can be

combined to form the “mass function”, which is

$$f_1(M_1, M_2) = \frac{K_1^3 P_{\text{orb}}}{2\pi G} (1 - e^2)^{3/2} = \frac{M_2^3 \sin^3 i}{(M_1 + M_2)^2}. \quad (1.5)$$

Here M_1 is the mass of the star being observed, M_2 is the mass of the other star, and i is the inclination of the binary orbit to our line of sight ($i = 0$ means a face-on orbit, $i = \pi/2$ means an edge-on orbit). From this expression, f_1 is the minimum possible mass for M_2 ; if $M_1 > 0$ or $i < \pi/2$ then $M_2 > f_1$. If periodically shifting spectral lines are also observed from the second star (and thus the binary is a so-called double-line spectroscopic binary), then the mass ratio is known and only i is uncertain.

The inclination can be constrained for eclipsing systems. Particular precision is possible in some extrasolar planet observations because of the Rossiter-McLaughlin effect (in which the apparent color of the star varies in a way dependent on inclination as a planet transits across its disk; see [147, 194]). This effect also produces a velocity offset, which might have been seen in 2S 0921–63 [110]. The inclination can also be constrained in systems for which the companion to a compact object just fills its Roche lobe. This is because as the companion orbits it presents different aspects to us, and the amplitude of variation depends on the inclination; for example, a star in a face-on orbit looks the same to us at all phases, whereas star in an edge-on orbit varies maximally in its aspect [13, 145]. In practice this analysis is limited to systems that have low-mass companions (because Roche lobe overflow from a high-mass companion to a lower-mass compact object is usually unstable; see [81]) and that have transient accretion phases and hence have long intervals in which there is effectively no accretion disk (because an active accretion disk easily outshines a low-mass star and thus the binary periodicity is very difficult to observe). Neutron star X-ray binaries might be less likely to be transient than black hole X-ray binaries, although the data are ambiguous on this point, and their companions tend to be much less massive and hence dimmer than the companions to black holes [81]. Thus despite the great success of this method for black hole binaries it has found limited application for neutron star binaries.

1.3.2 *Post-Keplerian Measurements of Pulsar Binaries*

The most precise measurements of the masses of neutron stars in binaries are made for systems in which additional parameters can be measured. The extreme timing precision of pulsars makes pulsar binaries especially good candidates for such measurements. The new effects that can be measured are:

- Precession of the pericenter of the system, $\dot{\omega}$.
- Einstein delay γ . At pericenter, the gravitational redshift from the system is maximized.

- Binary orbital decay \dot{P}_b . Gravitational waves are emitted by anything that has a time-variable quadrupole (or higher-order) mass moment. This shrinks and circularizes binary orbits.
- Shapiro delay, r and s . When the signal from the pulsar passes near its companion, time dilation in the enhanced potential delays the signal compared to the arrival time of a photon in flat spacetime. The magnitude of the delay over the orbit is characterized by the range r and shape s of the delay as a function of phase. See [83] for a recent reparameterization of the Shapiro delay that may represent the error region better for some orbital geometries.

Using the notation of [82], the dependences of these post-Keplerian parameters on the properties of the binary are

$$\begin{aligned}
 \dot{\omega} &= 3 \left(\frac{P_b}{2\pi} \right)^{-5/3} (T_\odot M)^{2/3} (1 - e^2)^{-1} \\
 \gamma &= e \left(\frac{P_b}{2\pi} \right)^{1/3} T_\odot^{2/3} M^{-4/3} m_c (m_p + 2m_c) \\
 \dot{P}_b &= -\frac{192\pi}{5} \left(\frac{P_b}{2\pi} \right)^{-5/3} f(e) T_\odot^{5/3} m_p m_c M^{-1/3} \\
 r &= T_\odot m_2 \\
 s &= \sin i
 \end{aligned} \tag{1.6}$$

where m_p is the pulsar mass, m_c is the companion mass, $M = m_p + m_c$ is the total mass (all masses are in units of a solar mass), $T_\odot = GM_\odot/c^3 = 4.925590947 \mu\text{s}$, and $f(e) = (1 + 73e^2/24 + 37e^4/96)(1 - e^2)^{-7/2}$. For a given system, there are thus three Keplerian parameters that can be measured (binary period, radial velocity, and eccentricity) along with the five post-Keplerian parameters. For a system such as the double pulsar J0737–3039A/B [47] additional quantities can be measured. Hence double neutron star systems in which at least one is visible as a pulsar are superb probes of general relativity and yield by far the most precise masses ever obtained for any extrasolar objects.

As discussed by Freire [82], the neutron stars with the greatest timing precision are the millisecond pulsars. These, however, are spun up by accretion in Roche lobe overflow systems, and that accretion also circularizes the system to high precision. As a result, precession of the pericenter and the Einstein delay cannot be measured. The Shapiro delay, however, can be measured even for circular binaries, and because the Shapiro delay does not have classical contributions from tides (unlike pericenter precession, for example), r and s can yield unbiased mass estimates. As pointed out by Scott Ransom, Shapiro delay measurements are likely to become more common due to the development of very high-precision timing for gravitational wave detection via pulsar timing arrays. The consequence is that currently the most constrained systems are field NS-NS binaries, in which little mass transfer has taken place in the system and the stars are thus close to their birth masses. In contrast, recycled millisecond pulsars have had an opportunity to acquire an additional several tenths of a solar mass via accretion.

Another possibility, which is described clearly by Freire [82], is that in high stellar density environments such as globular clusters binary-single interactions could play a major role. For example, a pulsar could be recycled to millisecond periods and then an exchange interaction could leave it in an eccentric binary with a white dwarf or another neutron star. Such a system would have a measurable $\dot{\omega}$ and γ , and the neutron star could be high-mass and have excellent timing precision.

We do note that there are two drawbacks to NS-WD systems in globulars compared to field NS-NS systems. First, although white dwarfs are small they are not point masses to the degree that neutron stars are. As a result, there is a small contribution to the precession from the finite structure of the white dwarfs. Second, even at the high stellar densities of globulars a comparatively large orbit is required for there to be a significant probability of interaction. To see this, note that the rate of interactions for a binary of interaction cross section σ is $\tau^{-1} = n\sigma v$, where n is the number density of stars (typically in the core $n = 10^5 - 10^6 \text{ pc}^{-3}$) and $v \sim 10 \text{ km s}^{-1}$ is the velocity dispersion. For a system of mass M , the interaction cross section for a closest approach of a , roughly equal to the semimajor axis of the binary, is $\sigma \approx \pi a(2GM/v^2 + a)$. If $M \approx 2 M_\odot$ and $n = 10^5 \text{ pc}^{-3}$, this implies $\tau = 10^{10} \text{ yr}$ when $a \approx 0.04 \text{ AU}$. This implies orbital periods greater than a day, so dynamically formed NS-WD binaries are systematically larger than NS-NS binaries formed in situ. Thus longer observation times are required to achieve a given precision.

1.3.3 *Dynamically Estimated Neutron Star Masses and Future Prospects*

For a recent compilation of dynamically estimated neutron star masses and uncertainties, see [115]. From the standpoint of constraints on dense matter, the most important development over the last few years has been the discovery of neutron stars with masses $M \sim 2 M_\odot$, and possibly more. The first such established mass was for PSR J1614–2230. Demorest et al. [72] determined that its mass is $M = 1.97 \pm 0.04 M_\odot$, which they obtained via a precise measurement of the Shapiro delay. This measurement was aided by the nearly edge-on orientation of the system (inclination angle 89.17°), which increases the maximum magnitude of the delay and produces a cuspy timing residual that is easily distinguished from any effects of an eccentric orbit.

The second large mass that has been robustly established belongs to PSR J0348+0432. Antoniadis et al. [11] observed gravitationally redshifted optical lines from the companion white dwarf. The observed Doppler modulation of the energy of these lines yields a mass ratio when combined with the modulation of the observed spin frequency of the pulsar. In addition, interpretation of the Balmer lines from the white dwarf in the context of white dwarf models gives a precise mass for the white dwarf, and indicates that the neutron star has a mass of $M = 2.01 \pm 0.04 M_\odot$.

In addition to these well-established high masses, there are hints that some black widow pulsars (those that are currently evaporating their companions) might have even higher masses. This was first reported for the original black widow pulsar PSR B1957+20 [223]. For this star the best-fit mass is $M = 2.40 \pm 0.12 M_\odot$, but at the highest allowed inclination and lowest allowed center of mass motion the mass could be as low as $1.66 M_\odot$. More recently, [188] analyzed the gamma-ray black widow pulsar PSR J1311–3430 and found a mass of $M = 2.7 M_\odot$ for simple heated light curves (but with significant residuals in the light curve), and no viable solutions with a mass less than $2.1 M_\odot$. They conclude that better modeling and more observation is needed to establish a reliable mass, but it is an intriguing possibility that black widow pulsars have particularly large masses.

From the astrophysical standpoint, it has been proposed that neutron star birth masses are bimodal, depending on whether the core collapse occurs due to electron capture or iron core collapse [197]. There is also mounting evidence for systematically higher masses in systems that are expected to have had substantial accretion [241]. From the standpoint of nuclear physics, [132] point out that $2.0 M_\odot$ neutron stars place interesting upper limits on the physically realizable energy density, pressure, and chemical potential. Higher masses would present even stronger constraints.

To a far greater extent than with the other constraints described in this review, we can be confident that the mere passage of time will greatly improve the mass measurements, and indeed all of the timing parameters. Table II of [68] shows that as a function of the total observation time T (assuming a constant rate of sampling), the fractional uncertainties in the post-Keplerian parameters scale as $\Delta\dot{\omega} \propto T^{-3/2}$, $\Delta\gamma \propto T^{-3/2}$, $\Delta\dot{P}_b \propto T^{-5/2}$, $\Delta r \propto T^{-1/2}$, and $\Delta s \propto T^{-1/2}$; for the r and s parameters the improvements are simply due to having more measurements, whereas the others improve faster with time because the effects accumulate. Particularly good improvement is expected for the NS-WD systems because as we describe above they have larger orbits and thus slower precession than NS-NS systems. There is thus reason to hope that additional high-mass systems will be discovered.

There are also planned observatories and surveys that will dramatically increase the number of known pulsars of all types, which will likely include additional NS-NS and NS-WD systems. An example of such a planned observatory is the Square Kilometer Array, which has been projected to increase our known sample of pulsars by a factor of ~ 10 . In addition, as [215] pointed out recently, future high-precision astrometry will be able to deconvolve the parallactic, proper, and orbital motion of the two components of a high-mass X-ray binary. They estimate that for parameters appropriate to the Space Interferometry Mission [201] this will yield a neutron star mass accurate to 2.5% in X Per, to 6.5% in Vela X-1, and to $\sim 10\%$ in V725 Tau and GX 301–2.

It is thus probable that in the next ~ 10 years we will have far more, and far better, estimates of the masses of individual neutron stars. We do not, however, have a guarantee that any of those masses will be close to the maximum allowed. We thus need additional ways to access the properties of high-density matter. In particular,

many equations of state imply similar maximum masses but widely different radii. We therefore turn to constraints on the radius.

1.4 Constraints on Radius, and Other Mass Constraints

As discussed in Sect. 1.2, accurate measurements of the radii of neutron stars would strongly constrain the properties of neutron star core matter. Unfortunately, all current inferences of neutron star radii are dominated by systematic errors, and hence no radius estimates are reliable enough for such constraints. However, future measurements using the approved missions NICER [90] and Athena+ [161] and the proposed missions LOFT [78] and AXTAR [185], and hold great promise for precise radius measurements if the effects of systematic errors can be shown to be small. In this section we discuss various proposed methods for measuring radii and the diverse results obtained by applying these methods. Some of the methods also result in mass estimates, so we discuss those implications along the way.

1.4.1 *Thermonuclear X-ray Bursts*

More than 30 years ago it was proposed that the masses and radii of neutron stars could be obtained via measurement of thermonuclear X-ray bursts [224]. These bursts occur when enough hydrogen or helium (or carbon for the long-lasting “superbursts”) accumulates on a neutron star in a binary. Nuclear fusion at the base of the layer becomes unstable, leading to a burst that lasts for seconds to hours. For a selection of observational and theoretical papers on thermonuclear bursts, see [23, 64, 85, 86, 91, 112, 125, 137, 204, 212, 213, 236]. In some bursts, fits of a Planck function to the spectra reveal a temperature that initially increases, then decreases, then increases again before finally decreasing [107, 136, 203]. These are called photospheric radius expansion (PRE) bursts [168]. The usual assumption is that PREs occur because the radiative luminosity exceeds the Eddington luminosity

$$L_E = \frac{4\pi G M c}{\kappa} \quad (1.7)$$

where M is the mass of the star and κ is the radiative opacity. At luminosities greater than L_E , an optically thick wind can be driven a potentially significant distance from the star. This leads to an increase in the radiating area and a consequent decrease in the temperature [75, 167]. For Thomson scattering in fully ionized matter with a hydrogen mass fraction X , $\kappa = 0.2(1 + X) \text{ cm}^2 \text{ g}^{-1}$ and thus

$$L_E = 2.6 \times 10^{38} \text{ erg s}^{-1} (1 + X)^{-1} (M/M_\odot) . \quad (1.8)$$

The basic method of [224] involves several assumptions. These are:

1. The full surface radiates uniformly after the photosphere has retreated to the radius of the star.
2. The stellar luminosity is the Eddington luminosity at the point of “touchdown”, which is defined as the time after the peak inferred photospheric radius is reached when the color temperature, derived from a Planck fit to the spectrum, is maximal. The luminosity can then be determined via measurement of the flux at Earth and the distance to the star, assuming that the flux is emitted isotropically.
3. The spectral model for the atmosphere is correct. Thus the model must have been verified against data good enough to distinguish between models, and the atmospheric composition must be known. It is typically assumed that the color factor $f_c \equiv T_{\text{col}}/T_{\text{eff}}$, which is the ratio between the fitted Planck temperature and the effective temperature, is not only known but is constant throughout the cooling phase.
4. All other sources of emission from the system are negligible.

Using these assumptions, and using the notation of [206], if we have measured the distance D to the star and know κ , we can measure the touchdown flux

$$F_{\text{TD},\infty} = \frac{GMc}{\kappa D^2} \sqrt{1 - 2\beta(r_{\text{ph}})} \quad (1.9)$$

where $\beta(r) \equiv GM/rc^2$, the factor before the square root is the Eddington flux diluted by distance, and r_{ph} is the radius of the photosphere. We can also use the cooling phase of the burst to define a normalized angular surface area

$$A = \frac{F_{\infty}}{\sigma_{\text{SB}} T_{\text{col},\infty}^4} = f_c^{-4} \left(\frac{R}{D} \right)^2 (1 - 2\beta)^{-1}. \quad (1.10)$$

Here $\sigma_{\text{SB}} = 5.6704 \times 10^{-5} \text{ erg cm}^{-2} \text{ s}^{-1} \text{ K}^{-4}$ is the Stefan-Boltzmann constant and F_{∞} and $T_{\text{col},\infty}$ are the flux and fitted Planck temperature that we measure in the cooling phase. Then the combinations of observed quantities

$$\begin{aligned} \alpha &\equiv \frac{F_{\text{TD},\infty}}{\sqrt{A}} \frac{\kappa D}{c^3 f_c^2} \\ \gamma &\equiv \frac{Ac^3 f_c^4}{F_{\text{TD},\infty} \kappa} \end{aligned} \quad (1.11)$$

can be related to β and R by $\alpha = \beta(1 - 2\beta)$ and $\gamma = R[\beta(1 - 2\beta)^{3/2}]^{-1}$ and solved to yield

$$\begin{aligned} \beta &= \frac{1}{4} \pm \frac{1}{4} \sqrt{1 - 8\alpha}, \\ R &= \alpha \gamma \sqrt{1 - 2\beta}, \\ M &= \beta R c^2 / G. \end{aligned} \quad (1.12)$$

The problem is that for several bursters, the most probable values of the observationally inferred quantities $F_{\text{TD},\infty}$, A , and D , combined with the model parameter f_c , yield $\alpha > 1/8$. This would imply that the mass and radius are complex numbers. For example, in their analysis of 4U 1820–30, [95] used a Gaussian prior probability distribution for $F_{\text{TD},\infty}$, which had a mean $F_0 = 5.39 \times 10^{-8} \text{ erg cm}^{-2} \text{ s}^{-1}$ and a standard deviation $\sigma_F = 0.12 \times 10^{-8} \text{ erg cm}^{-2} \text{ s}^{-1}$. They also used a Gaussian prior probability distribution for A , with $A_0 = 91.98 (\text{km}/10 \text{ kpc})^2$ and $\sigma_A = 1.86 (\text{km}/10 \text{ kpc})^2$. Their prior probability distribution for D was a boxcar distribution with a midpoint $D_0 = 8.2 \text{ kpc}$ and a half-width of $\Delta D = 1.4 \text{ kpc}$. Finally, they assumed a boxcar prior probability distribution for the color factor, with $f_{c0} = 1.35$ and a half-width $\Delta f_c = 0.05$. If we take the midpoint of each distribution and also follow [95] by assuming that the opacity is dominated by Thomson scattering and thus $\kappa = 0.2 \text{ cm}^2 \text{ g}^{-1}$ for the pure helium composition appropriate to 4U 1820–30, we find $\alpha = 0.179 > 1/8$.

Güver et al. [95] note that the probability of obtaining a viable M and R for 4U 1820–30 from these equations drops with increasing distance, but if we reduce D to the 6.8 kpc, which is the smallest value allowed in the priors of [95], and keep the other input parameters fixed, we find $\alpha = 0.148$. If we also increase f_c to its maximum value of 1.4 and take the $+2\sigma$ value of A and the -2σ value of $F_{\text{TD},\infty}$, α is still 0.129. In fact [206] showed that if we consider the prior probability distribution of $F_{\text{TD},\infty}$, A , D , and f_c used by Güver et al. [95], only a fraction 1.5×10^{-8} of that distribution yields real numbers for M and R . This demonstrates that the 4% fractional uncertainties on the mass and radius of this neutron star obtained by Güver et al. [95] emerge from the theoretical assumptions rather than from the data. Thus such apparent precision is actually a red flag that one or more of the model assumptions is incorrect.

The first suggestion for which assumption is in error came from [206], who proposed that although the entire surface still emits uniformly throughout the cooling phase, the photospheric radius might be larger than the radius of the star, i.e., $r_{\text{ph}} > R$. However, analysis of the cooling phase of the superburst from 4U 1820–30 [158] demonstrates that such a solution is disallowed for at least the superburst emission from this star, because any detectable change in photospheric radius would require a flux very close to Eddington, and such fluxes give extremely poor fits to the data. The work of [158] used and verified the fully relativistic Comptonized spectral models of [211], and also showed that the *fraction* of the surface that emits changes systematically throughout the superburst (the emitting area drops by $\sim 20\%$ during the $\sim 1600 \text{ s}$ analyzed). Moreover, there is no guarantee that the whole surface was emitting at *any* time. Thus the star does not emit uniformly over its entire surface during the superburst, and hence it cannot be assumed that it has uniform emission during shorter bursts when the data quality is insufficient to check this assumption. Indeed, the presence of burst oscillations (see [230] for a recent review) demonstrates that there is nonuniformity in burning during many bursts. Additional concerns are that the color factor is likely to evolve during the burst, and that some of the bursts are not fit well using existing spectral models [43, 55, 87, 89, 210, 242].

Suleimanov et al. [210] find a radius of more than 14 km from a long PRE burst from 4U 1724–307 based on fits of their spectral models to the decaying phase of the burst. As part of their fits, they find that the Eddington flux occurs not at touchdown, but at a 15% lower luminosity; this, therefore, calls into question another of the assumptions in the standard approach to obtaining mass and radius from bursts. Their radius value is based on the good fit they get to the bright portion of the burst, when according to their fits the local surface flux exceeds $\sim 50\%$ of Eddington. This is an intriguing method that should be considered carefully when data are available from the next generation of X-ray instruments. However, a potential concern is that the spectra does not agree with their models below $\sim 50\%$ of Eddington. This suggests that there is other emission in the system at least at those lower luminosities, and hence that some of this emission might be present at higher luminosities as well. Against this is the excellent fit without extra components that [158] obtained for the superburst from 4U 1820–30 using the models of [211]. More and better data are the key.

If truly excellent spectra can be obtained, then as pointed out by [143], inference of the surface gravity g and surface redshift z leads uniquely to determination of the stellar mass and radius. However, even the $\sim 2 \times 10^7$ counts observed using *RXTE* from the 4U 1820–30 superburst are insufficient to determine both g and z uniquely [158], so this appears to require much larger collection areas. The combination $(1+z)/g^{2/9}$ can be measured precisely using sufficiently good continuum spectra, and then combined with other measurements to, possibly, constrain M and R [138, 158], so this is promising for the future. The net result is that currently inferred masses and radii from spectral fits to thermonuclear X-ray bursts must be treated with caution; none are reliable enough to factor into equation of state constraints.

1.4.2 Fits of Thermal Spectra to Cooling Neutron Stars

In principle, observations of cooling neutron stars with known distances allow us to measure the radii of those stars, modulo an unknown redshift. In practice, as with radius estimates from bursts, systematic errors dominate and thus current radius determinations are not reliable enough to help constrain the properties of dense cold matter.

To understand the basic principles, suppose that the star is at a distance d and that we measure a detector bolometric flux $F_{\text{det,bol}}$ from the star that is fit by a spectrum with an effective temperature $T_{\text{eff},\infty}$ at infinity. Suppose that we also assume that the entire surface radiates uniformly. If the surface redshift is z then the luminosity at the surface is $L_{\text{surf}} = (1+z)^2 L_{\infty} = (1+z)^2 F_{\text{det,bol}} 4\pi d^2 = 4\pi R^2 \sigma_{\text{SB}} T_{\text{surf}}^4 = 4\pi R^2 (1+z)^4 \sigma_{\text{SB}} T_{\text{eff},\infty}^4$. This implies

$$R = (1+z)^{-1} d [F_{\text{det,bol}} / (\sigma_{\text{SB}} T_{\text{eff},\infty}^4)]^{1/2}. \quad (1.13)$$